Aalborg Universitet

AALBORG UNIVERSITY
DENMARK

The Effect of Pulsed Current on the Lifetime of Lithium-ion Batteries

Huang, Xinrong; Jin, Siyu; Meng, Jinhao; Teodorescu, Remus; Stroe, Daniel-Ioan

The Effect of Pulsed Current on the Lifetime of Lithium-ion Batteries

Xinrong Huang[1], Siyu Jin[1], Jinhao Meng[2], Remus Teodorescu[1], and Daniel-Ioan Stroe[1]

[1] *Department of Energy Technology*, *Aalborg University*, Aalborg, Denmark
[2] *School of Automation Engineering*, *University of Electronic Science and Technology of China*, Chengdu, China
hxi@et.aau.dk, sji@et.aau.dk, jinhao@scu.edu.cn, ret@et.aau.dk, dis@et.aau.dk

Abstract—**The pulsed current charging technique has been proposed to improve the charging performance and lifetime of Lithium-ion batteries. However, the optimal operating conditions of the pulsed current, e.g., profile, frequency, duty cycle, and amplitude, still need to be investigated. This work focuses on investigating the effect on the lifetime of Lithium-ion battery cells of the positive pulsed current (PPC) in the low-frequency range between 0.05 Hz and 1 Hz. According to the results of cycling aging tests, the PPC charging at 0.05 Hz can extend the lifetime up to 60% compared with the traditional constant current (CC) charging. Furthermore, a lifetime model of the battery cell in terms of the capacity fade and the increase in internal resistance is developed to estimate the effect of the PPC charging at different frequencies on the lifetime of the Lithium-ion battery cells.**

Index Terms—**Lithium-ion battery, lifetime, pulsed current charging, frequency.**

I. Introduction

To alleviate the environmental issues caused by greenhouse gas emissions, electric vehicles (EVs) are actively promoted and are expected to gradaully replace traditional internal combustion engine cars [1]. The Lithium-ion battery technique has been widely used in EVs due to its high energy density and low self-discharging rate [2]. Two issues affect the penetration rate of EVs, i.e., the long charging time and the reduced lifetime of Lithium-ion batteries. Three charging levels are considered for EVs [3]. The first charging level uses the standard three-prong plug, which are designed for household scenarios. The charging time of this level is around 10-12 hours, and the EVs usually need to be charged overnight. Level 2 increases the power level, and the charging time of EVs is shortened by half of Level 1, which is around 2-6 hours. Level 3 is defined as the fast charging level, and the charging time is limited to 30 minutes [4]. However, regardless of the charging level, the charging time is much longer than the time that the internal combustion engine cars fill up. The battery lifetime is another challenge because it is directly connected with the EV cost [5], [6]. Therefore, it is necessary to develop advanced charging strategies to tackle these two challenges. The common-used EV battery charging method is constant current (CC) charging. The batteries charged by the CC with a lower C-rate will obtain a longer lifetime [7]; however, the charging time will increase proportionally. Therefore, achieving a tradeoff between the charging time and lifetime has been a target of various studies in this research field.

Pulse current charging technique has been proposed to improve the discharging capacity, charging efficiency, and charging speed [8], [9]. Negative pulsed current (NPC) and positive pulsed current (PPC) are the two basic modes of the pulsed current charging [10]. A period of the NPC consists of a positive pulse, a negative pulse, and a relaxation time. In [11], the NPC charging can extend the Lithium-ion battery lifetime by 128% when compared with the constant current-constant voltage (CC-CV) charging. In [12], the Lithium-ion battery cells charged by the NPC at 0.046 Hz and 0.023 Hz can extend their lifetime by 17% when compared with the CC-CV charging. However, due to the discharging pulses during the charging process, the charging efficiency of the NPC is lower than that of the CC by 10% [12].

The PPC mode is the positive pulse followed by a relaxation time [13]. In [14], Lithium-ion battery cells charged by the PPC with optimal parameters (i.e., 12.5-kHz frequency, 50% duty cycle, and 25-°C ambient temperature) can extend the lifetime by 100 cycles when compared with the CC-CV charging. Furthermore, the charging speed and the charging efficiency can also be improved by 47.6% and 11.3% [15], [16]. However, the comparison between the PPC charging without CV phase and the CC charging with CV phase is not fair because the CV phase would have a significant impact on the lifetime, charging time, and discharging capacity for Lithium-ion batteries. In [17], the capacity utilization and charging time of the PPC at 1 Hz and 25 Hz are similar to that of the CC-CV charging. In [18], the 0.02-Hz PPC-CV can improve capacity retention slightly by 0.26% when compared to the CC charging.

The existing research of the PPC charging mostly focuses on the high-frequency range (i.e., 1-100k Hz) and does not show a significant advantage in lifetime extention. Therfore, the effect of PPC charging at low-frequency range on Lithium-ion batteries needs to be investigated and discussed. The effect of the low-frequency PPC charging on battery performance, which includes the charging capacity, charging time, and the maximum rising temperature, has been studied in our previous work [19], [20]. In this work, the impact of low-frequency PPC on battery lifetime is investigated. Based on the obtained results of the capacity fade and the changes in the internal

resistance, a battery lifetime model based on the PPC charging is developed and parameterized.

This paper is structured as follows. Section II provides the entire testing procedure. Section III presents the experimental results and the lifetime model of the Lithium-ion battery cell based on the PPC charging. Section IV gives the conclusions.

II. EXPERIMENT

A. Battery cell

The main electrical parameters of the LiNiMnCo(NMC)-based battery cells used for the investigation are summarized in Table I. All the experiments are performed using a Digatron battery test station. During all the tests, the cells are placed in a Memmert climate chamber to ensure a stable and reliable temperature. Fig. 1 shows an NMC cell under testing in the chamber.

TABLE I
MAIN PARAMETERS OF THE TESTED NMC BATTERY CELLS.

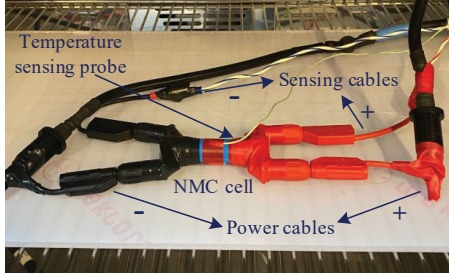| Parameter	Value
Nominal capacity Q_n, [Ah]	2.2
Nominal voltage V_n, [V]	3.6
Maximum voltage V_{max}, [V]	4.2
Minimum voltage V_{min}, [V]	2.5
Maximum (dis)charge current I_{max}, [A]	6.6
Operating temperature for charging Temp, [°C]	0-55

Fig. 1. An NMC battery cell during the test.

B. Positive Pulsed Current (PPC)

The current profile investigated in this work is the PPC, as shown in Fig. 2. The amplitude of the positive pulse is I_p. The period T_p of the PPC can be calculated by $1/f$, where f is the frequency of the PPC. The pulsed charging time and the relaxation time are represented as t_p and t_r, respectively. The duty cycle of the pulsed current D can be determined as follows:
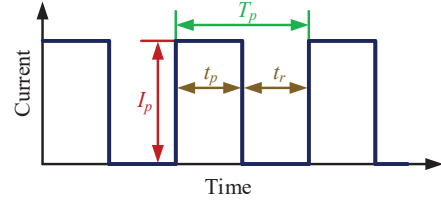
$$D = \frac{t_p}{T} \qquad (1)$$

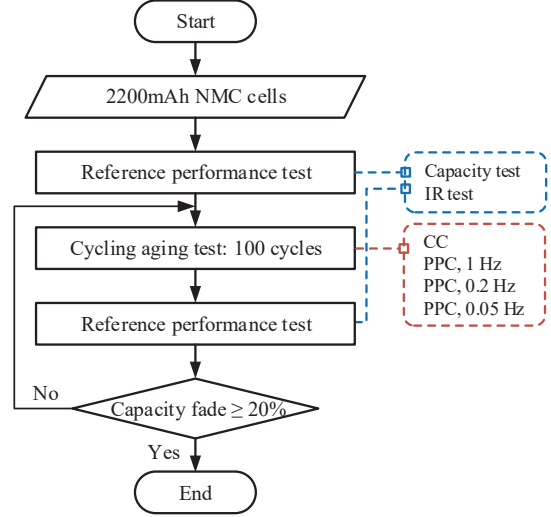Fig. 2. Schematic of the Positive Pulsed Current (PPC).

Fig. 3. Aging test procedures.

C. Test procedure

The aging test consists of the reference performance test and the cycling aging test, as shown in Fig. 3.

The performance test is performed before starting the cycling aging test and then performed after every 100 aging cycles until the battery cell reaches its end of life, i.e., a capacity fade of 20%. The reference performance test includes the capacity test and the internal resistance test, and both of them are performed at 25 °C. The internal resistance is obtained by the dc pulse technique. The procedure of the reference performance tests that were repeated for all tested cells are presented as follows:

1) Relaxation of the battery cell for one hour at 25 °C.;
2) Full charging of the battery cell by applying the CC-CV procedure with a current of 1 C; the charging process is finished when the current decreases to 5% of the nominal capacity of the battery cell;
3) Relaxation of the battery cell for one hour;
4) Full discharging of the battery cell by applying a 1-C current; the obtained discharging capacity is regarded as the battery current capacity;
5) Relaxation of the battery cell for one hour;
6) Full charging of the cell by applying a CC-CV pattern, which is the same as step 2;
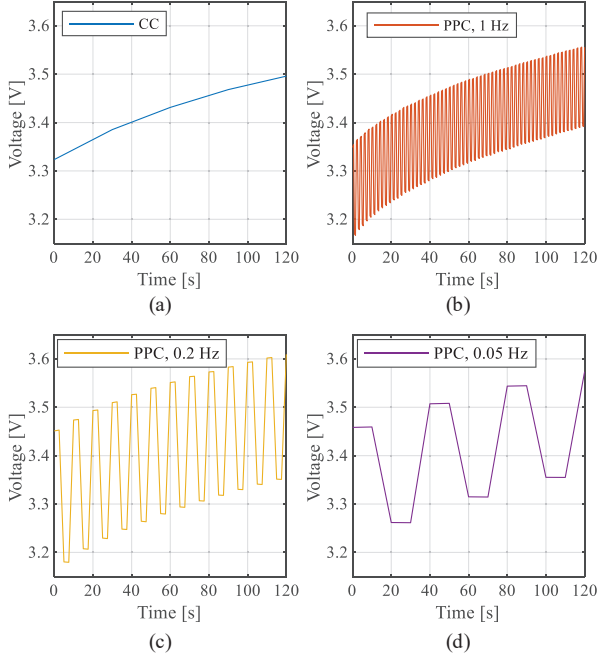7) Relaxation of the battery cell for 15 minutes;

Fig. 4. Examples of voltage profiles for the four charging current conditions: (a) CC, (b) PPC at 1 Hz, (c) PPC at 0.2 Hz, and (d) PPC at 0.05 Hz.

8) The following procedures are repeated for the internal resistance measurement at different SOCs, i.e., 10%, 30%, 50%, 70%, and 90%:

   a) Discharging the battery cell to the considered SOC;
   b) Charging of the battery cell by a 1-C current pulse for 18 seconds;
   c) Relaxation of the battery cell for 15 minutes;
   d) Discharging of the battery cell by a 1-C current pulse for 18 seconds;
   e) Relaxation of the battery cell for 15 minutes;

The capacity fade of the battery cell Q_{fade} can be determined by (2):

$$Q_{fade} = (1 - \frac{Q_N}{Q_{init}}) \cdot 100\% \qquad (2)$$

where N is the cycle number, Q_{init} is the initial capacity of the battery cell, and Q_N is the capacity of the battery cell during the cycling aging process, which can be obtained by step 4 of the reference performance test procedure.

The internal resistance IR can be determined as:

$$IR = \frac{\Delta V_{18s}}{I_{dc}} \qquad (3)$$

where ΔV_{18s} is the change in voltage during the 18-s dc pulse, and I_{dc} is the amplitude of the dc pulse. The internal resistance will increase with the aging process of the battery cell. The percentage increase of the internal resistance $IR_{icr.}$ can be calculated by (4):

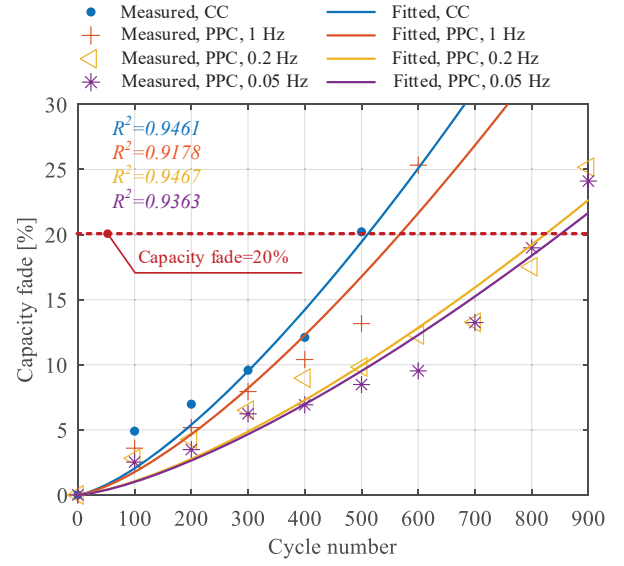$$IR_{icr.} = (\frac{IR_N}{IR_{init}} - 1) \cdot 100\% \qquad (4)$$

Fig. 5. Measured and fitted capacity fade of the tested cells cycled using both the CC and PPC charging.

To accelerate the aging process, the cycling aging tests are performed at 35 °C. The considered frequencies in this work are 0.05 Hz, 0.2 Hz, and 1 Hz. The duty cycle of the PPC is 50%. To ensure the same average charging current, the current amplitude of PPC and CC are 2 C (i.e., 4.4 A) and 1 C (i.e., 2.2 A), respectively; and the discharging current for both CC and PPC charging is 2 C. The voltage response profiles of the battery corresponding to different charging currents are shown in Fig. 4.

III. RESULTS AND DISCUSSION

A. Capacity fade

Fig. 5 shows the capacity fade of the NMC battery cells cycled using both CC and PPC charging. The battery cell aged by the CC charging reaches a capacity fade of 20% after 500 cycles. The battery cells cycled by the PPC charging at 1 Hz, 0.2 Hz, and 0.05 Hz reach 20% capacity fade after 600 cycles, 900 cycles, and 900 cycles. Moreover, the capacity fade of the PPC at 0.05 Hz is lower than that of 0.2 Hz by 1% after 900 cycles. With the increase in the cycle number, the capacity fade function for both CC and PPC charging can be obtained as:

$$Q_{fade}(N)[\%] = a \cdot N^{1.4} \qquad (5)$$

where a is the fitting coefficient, which depends on the charging current used for the cycling aging tests. The accuracy of the fitting was quantified by the R^2 coefficient. The capacity fade lifetime model of the NMC battery cell aged by the CC charging was found as follows:

$$Q_{fade.CC}(N)[\%] = 0.003236 \cdot N^{1.4} \qquad (6)$$

For the PPC charging, the fitting coefficient a_f depends on the pulse frequency:

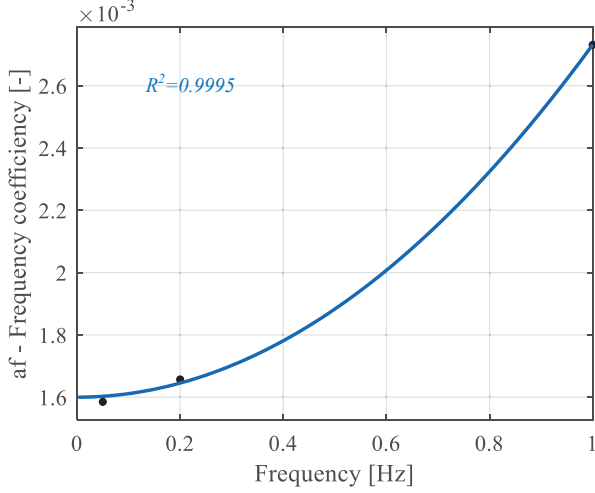$$Q_{fade}(N)[\%] = a_f \cdot N^{1.4} \qquad (7)$$

Fig. 6. Relationship between the a_f coefficient and the frequency of the PPC charging.
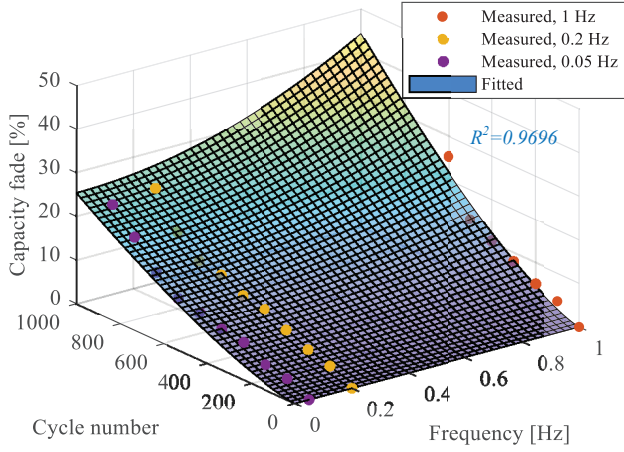

Fig. 7. Measured and fitted capacity fade based on the obtained lifetime model considering the frequency of the PPC charging.

To find a function that can estimate the capacity fade of the PPC charging with different frequencies, the dependence of the a_f coefficient on the frequency had to be found as presented in Fig. 6. The relationship between the a_f coefficient and the frequency can be expressed as (8). By introducing (8) in (9), the capacity fade lifetime model of the NMC battery cells for different frequencies of the PPC charging was obtained and is given in (9).

$$a_f = 0.0012 \cdot f^2 + 0.0016 \qquad (8)$$

$$Q_{fade}(f,N)[\%] = (0.0012 \cdot f^2 + 0.0016) \cdot N^{1.4} \qquad (9)$$

Based on the capacity fade lifetime model (9), the lifetime of the NMC battery cells considering different pulse charging frequency values was obtained, as shown in Fig. 7. The colored surface is the fitted capacity fade at different cycle numbers and frequencies, and the marked points are the measured capacity fade at different conditions.
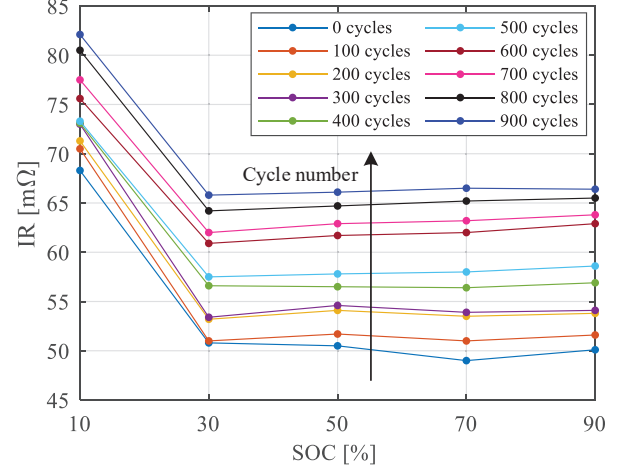

Fig. 8. Measured internal resistance of the battery cell aged with the PPC charging at 0.05 Hz.

B. Internal Resistance

The average value of the charging and discharging internal resistances is considered as the battery internal resistance at the corresponding SOC. Fig. 8 shows the internal resistance evolution of the cells cycled using the 0.05-Hz PPC charging. The internal resistance of the battery cell at 10% SOC is higher than that of other SOC conditions when the cycle number is consistent. Moreover, internal resistance is quasi-indepedent on SOC for SOCs between 30% and 90%, independent on the aging state; thus, in the following part, the IR lifetime modeling is performed only for 10% and 50% SOC. Fig. 9 shows the increase in IR at 10% and 50% SOCs during the aging tests. The IR increase of the battery cell aged by the CC charging is higher than that of the PPC charging. Moreover, a lower frequency of PPC charging has a slower IR increase for both 50% and 10% SOCs. Therefore, the degradation in the IR is consistent with the capacity fade of the NMC cells.

The same algorithm used for the capacity fade was followed to express the IR increase of the NMC battery cells with increasing cycle number. The IR lifetime model of the NMC cell aged by the CC charging was found as follows:

$$IR_{icr.CC}(N)[\%] = 0.006145 \cdot N^{1.4} \qquad (10)$$

The dependence of the b_f coefficient on the frequency is presented in Fig. 10. The relationship between the b_f coefficient and the pulse frequency can be expressed as (11) and (12):

$$b_{f.10} = -0.05 \cdot f^{-0.0041} + 0.052 \qquad (11)$$

$$b_{f.50} = -0.05 \cdot f^{-0.013} + 0.05465 \qquad (12)$$

where $b_{f.10}$ and $b_{f.50}$ are the frequency coefficienct at 10% and 50% SOCs, respectively. Then, the IR lifetime model of the NMC battery cells for different frequencies of the PPC charging was developed as:

$$IR_{icr.10}(f,N)[\%] = (-0.05 \cdot f^{-0.0041} + 0.052) \cdot N^{1.4} \qquad (13)$$

$$IR_{icr.50}(f,N)[\%] = (-0.05 \cdot f^{-0.013} + 0.05465) \cdot N^{1.4} \qquad (14)$$
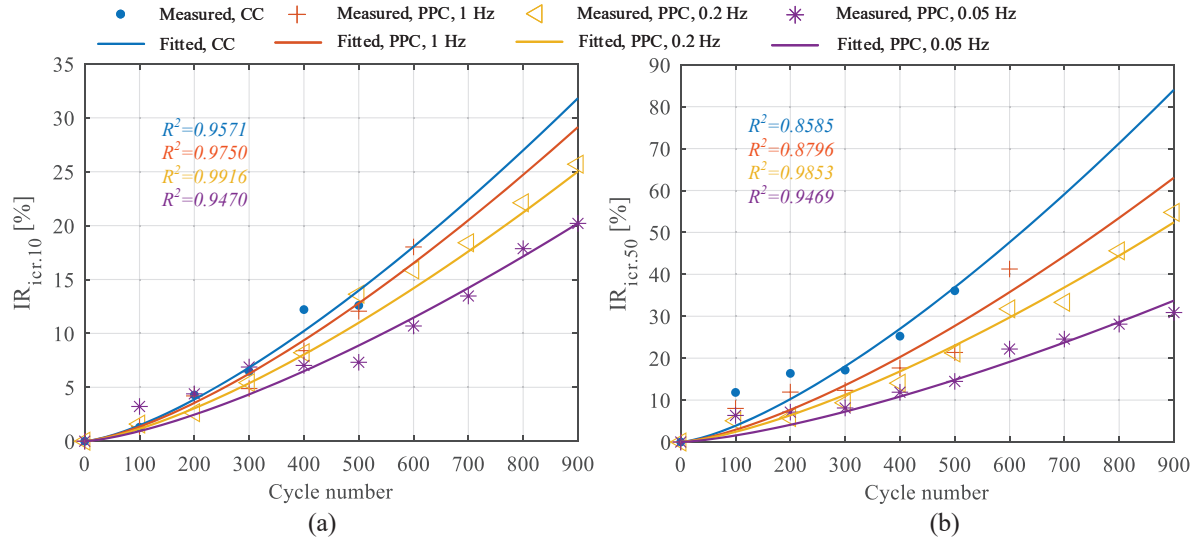
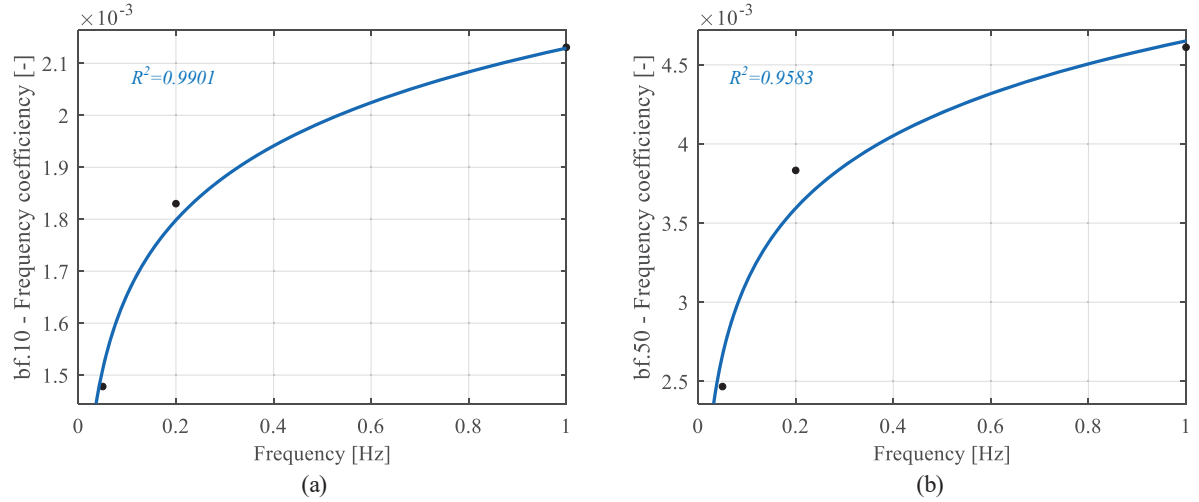Fig. 9. Measured and fitted internal resistances: (a) SOC=10% and (b) SOC=50%.

Fig. 10. Relationship between the b_f coefficient and the frequency of the PPC: (a) SOC=10% and (b) SOC=50%.

Accordingly, the IR increase at different number of cycles and frequencies is presented for 10% SOC and 50% SOC in Fig. 11(a) and Fig. 11(b), respectively. The surface represents the IR increase lifetime model, while he marked points are the measured IR points at various cycle numbers and frequencies.

C. Summary

According to the experimental results, the effect of the PPC charging on the NMC battery cells can be summarized as follows:

- The PPC charging can extend the battery lifetime up to 60% compared with the CC charging.
- A lower frequency of the PPC charging can obtain a longer battery lifetime in the investigated frequency range, i.e., between 0.05 Hz and 1 Hz.

- The difference in the impact on the capacity fade decreases with the decrease in the frequency. For example, the capacity fade of the 0.2-Hz and the 0.05-Hz PCC charging are 25.2% and 24.1%, respectively, after 900 cycles.
- The PPC charging can slow down the increase in IR compared with the CC charging. Moreover, a lower frequency of the PPC charging will obtain a lower IR increase.
- The degradation of the IR is consistent with the capacity fade of the NMC battery cells.

Therefore, PPC charging can be considered as an advanced charging strategy for the lifetime extension of Lithium-ion batteries.
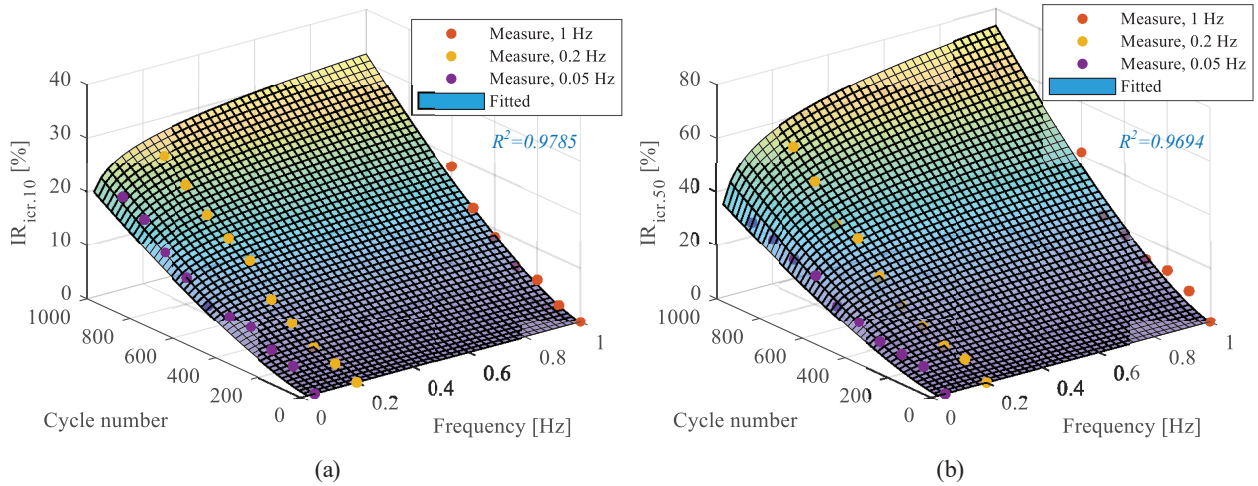
Fig. 11. Measured and fitted IR increase based on the proposed IR lifetime model considering the frequency of the PPC charging: (a) SOC=10% and (b) SOC=50%.

IV. CONCLUSION

This paper experimentally investigated the effect of low-frequency PPC charging on the lifetime of NMC battery cells. The considered frequency of the PPC charging in this work is 0.05 Hz, 0.2 Hz, and 1 Hz. The experimental results illustrated that the PPC charging can extend the lifetime by up to 60% compared with the CC charging. Furthermore, a lower frequency of the PPC charging will obtain a lower capacity fade in the considered frequency range. The changes in IR are consistent with the degradation of the capacity of the NMC battery cells. According to the experimental results, the lifetime model in terms of the capacity fade and IR increase has also been developed and parameterized.

REFERENCES

[1] J. Meng, L. Cai, D.-I. Stroe, X. Huang, J. Peng, T. Liu, and R. Teodorescu. An automatic weak learner formulation for lithium-ion battery state of health estimation. *IEEE Trans. Ind. Electron.*, pages 1–1, 2021.

[2] X. Huang, X. Sui, D.-I. Stroe, and R. Teodorescu. A review of management architectures and balancing strategies in smart batteries. In *IECON 2019 - 45th Annual Conference of the IEEE Industrial Electronics Society*. IEEE, Oct. 2019.

[3] S. S. Williamson, A. K. Rathore, and F. Musavi. Industrial electronics for electric transportation: Current state-of-the-art and future challenges. *IEEE Trans. Ind. Electron.*, 62(5):3021–3032, May 2015.

[4] M. Yilmaz and P. T. Krein. Review of battery charger topologies, charging power levels, and infrastructure for plug-in electric and hybrid vehicles. *IEEE Trans. Power Electron.*, 28(5):2151–2169, May 2013.

[5] J. Meng, L. Cai, D.-I. Stroe, J. Ma, G. Luo, and R. Teodorescu. An optimized ensemble learning framework for lithium-ion battery state of health estimation in energy storage system. *Energy*, 206:118140, Sep. 2020.

[6] Z. Hua, Z. Zheng, E. Pahon, M.-C. Péra, and F. Gao. Remaining useful life prediction of PEMFC systems under dynamic operating conditions. *Energy Conversion and Management*, 231:113825, Mar. 2021.

[7] M. Dubarry, C. Truchot, B. Y. Liaw, K. Gering, S. Sazhin, D. Jamison, and C. Michelbacher. Evaluation of commercial lithium-ion cells based on composite positive electrode for plug-in hybrid electric vehicle applications. part II. degradation mechanism under 2c cycle aging. *J. Power Sources*, 196(23):10336–10343, Dec. 2011.

[8] L.-R. Chen, J.-J. Chen, N.-Y. Chu, and G.-Y. Han. Current-pumped battery charger. *IEEE Trans. Ind. Electron.*, 55(6):2482–2488, Jun. 2008.

[9] L.-R. Chen, C.-M. Young, N.-Y. Chu, and C.-S. Liu. Phase-locked bidirectional converter with pulse charge function for 42-v/14-v dual-voltage PowerNet. *IEEE Trans. Ind. Electron.*, 58(5):2045–2048, May 2011.

[10] X. Huang, Y. Li, A. B. Acharya, X. Sui, J. Meng, R. Teodorescu, and D.-I. Stroe. A review of pulsed current technique for lithium-ion batteries. *Energies*, 13(10):2458, May 2020.

[11] J. Li, E. Murphy, J. Winnick, and P. A Kohl. The effects of pulse charging on cycling characteristics of commercial lithium-ion batteries. *J. Power Sources*, 102(1-2):302–309, Dec. 2001.

[12] M. Abdel-Monem, K. Trad, N. Omar, O. Hegazy, P. V. Bossche, and J. V. Mierlo. Influence analysis of static and dynamic fast-charging current profiles on ageing performance of commercial lithium-ion batteries. *Energy*, 120:179–191, Feb. 2017.

[13] L.-R. Chen, S.-L. Wu, D.-T. Shieh, and T.-R. Chen. Sinusoidal-ripple-current charging strategy and optimal charging frequency study for li-ion batteries. *IEEE Trans. Ind. Electron.*, 60(1):88–97, Jan. 2013.

[14] J. Amanor-Boadu, A. Guiseppi-Elie, and E. Sánchez-Sinencio. The impact of pulse charging parameters on the life cycle of lithium-ion polymer batteries. *Energies*, 11(8):2162, Aug. 2018.

[15] J. M. Amanor-Boadu, A. Guiseppi-Elie, and E. Sanchez-Sinencio. Search for optimal pulse charging parameters for li-ion polymer batteries using taguchi orthogonal arrays. *IEEE Trans. Ind. Electron.*, 65(11):8982–8992, Nov. 2018.

[16] J. M. Amanor-Boadu, M. A. Abouzied, and E. Sanchez-Sinencio. An efficient and fast li-ion battery charging system using energy harvesting or conventional sources. *IEEE Trans. Ind. Electron.*, 65(9):7383–7394, Sep. 2018.

[17] P. Keil and A. Jossen. Charging protocols for lithium-ion batteries and their impact on cycle life—an experimental study with different 18650 high-power cells. *J. Energy Storage*, 6:125–141, May 2016.

[18] H. Lv, X. Huang, and Y. Liu. Analysis on pulse charging–discharging strategies for improving capacity retention rates of lithium-ion batteries. *Ionics*, 26(4):1749–1770, Jan. 2020.

[19] X. Huang, Y. Li, J. Meng, X. Sui, R. Teodorescu, and D.-I. Stroe. The effect of pulsed current on the performance of lithium-ion batteries. In *2020 IEEE Energy Conversion Congress and Exposition (ECCE)*. IEEE, Oct. 2020.

[20] V. Knap, T. Zhang, D. I. Stroe, E. Schaltz, R. Teodorescu, and K. Propp. Significance of the capacity recovery effect in pouch lithium-sulfur battery cells. *ECS Transactions*, 74(1):95–100, Dec. 2016.

[21] M. Uno and K. Tanaka. Influence of high-frequency charge–discharge cycling induced by cell voltage equalizers on the life performance of lithium-ion cells. *IEEE Trans. Veh. Technol.*, 60(4):1505–1515, May 2011.